The impeding effect of dissolved oxygen on the photocatalytic reduction of $[\text{PdCl}_n(\text{H}_2\text{O})_{4-n}]^{2-n}$ $(n=0\text{–}4)$ complexes employing different TiO_2 photocatalysts in the absence of an added sacrificial reducing agent

F. Mahlamvana, R.J. Kriek*

PGM Group, Research Focus Area for Chemical Resource Beneficiation (CRB), North-West University, Private Bag X6001, Potchefstroom 2520, South Africa

ABSTRACT

The photocatalytic reduction of chloro-aqua palladium(II) complexes, $[\text{PdCl}_n(\text{H}_2\text{O})_{4-n}]^{2-n}$ $(n=0\text{–}4)$, as a means of palladium metal recovery and waste water purification, was investigated employing four different titanium dioxide samples in a batch reactor. These suspensions were subjected to UV irradiation in the absence of an added sacrificial reducing agent (SRA) for oxygen purged, air equilibrated and nitrogen purged solutions. A commercial Degussa P25 titanium dioxide powder (DP25) was taken as standard photocatalyst and compared to three other commercial titanium dioxide powders, namely Tioxide A-HR (AHR), Sigma–Aldrich Anatase (SAA) and Sigma–Aldrich Rutile (SAR). The highest rate of photocatalytic reduction was observed for the lower chlorinated Pd(II) complexes in nitrogen, i.e. oxygen depleted solutions, at constant temperature, photocatalyst load, pH and ionic strength on all four photocatalysts. Sigma–Aldrich Rutile (SAR) was the only photocatalyst capable of reducing the highly chloride coordinated $[\text{PdCl}_4]^{2-}$ complex, in the absence of an added organic SRA, in air equilibrated and nitrogen purged solutions. The presence of dissolved oxygen was found to be detrimental to the photocatalytic reduction of highly chloride coordinated chloro-aqua palladium(II) complexes. The effect of the structure of the complex as well as the photocatalyst surface area, crystal phase composition, aggregate particle size and band gap energy was explored in an effort to elucidate the observed differences in behaviour of the photocatalysts.

1. Introduction

Palladium is today one of the most important noble metals and finds application in a diverse array of sectors. These include catalytic converters within the automotive sector, jewellery products, electronics, the dental sector and as catalyst in various chemical industries. Due to its versatility as catalyst palladium is used, for example, for hydrogenation and oxidation reactions [1–4]. Given their scarcity and economic value the noble metals have experienced a continued growth with regard to their recovery and recycling. Although recycling of palladium was forecast to decrease by 4% in 2012 (down to 2.24 million ounces), in response to autocatalyst collectors holding on to their scrap until prices improved, continued growth in the sale of the number of vehicles that contain palladium in their converters, which will ultimately be available for recycling, points towards a longer-term increase in the recovery of the metal from spent converters [5]. Several mainstream

hydrometallurgical methods are employed today for the recovery of palladium metal, which include leaching, selective precipitation, ion exchange and solvent extraction [6–8]. It is well known that the recovery and separation chemistry of palladium relies heavily on its chloride complexes as palladium(II) forms quite stable complexes with chloride [9–11]. These complexes are assumed to be square planar and can be represented by the general formula $[\text{PdCl}_n(\text{H}_2\text{O})_{4-n}]^{2-n}$ $(n=0\text{–}4)$ [12–14]. Wastewaters, resulting from mainstream recovery processes, generally contain precious metals in low concentration (ppm range) and to that regard concentration processes are essential. These concentration processes are again mainstream hydrometallurgical processes and their success is based on the successful manipulation of the chloro-aqua complexes of palladium(II) [15–17]. Compared to the traditional hydrometallurgical processes, for the recovery of dissolved noble metals from aqueous solution, the photocatalytic reduction of these dissolved metals to their metallic state is certainly a non-traditional method of recovery. In general it is accepted that the recovery of palladium(II) from solution, by means of photocatalytic reduction, necessitates the presence of a sacrificial reducing agent (SRA) [18–22]. Up to now this has certainly been true for metals that

* Corresponding author. Tel.: +27 (0)18 299 2345.
E-mail address: cobus.kriek@nwu.ac.za (R.J. Kriek).

Table 1
Physicochemical properties of four commercial titanium dioxide powders.

Characterisation method	TiO$_2$ photocatalyst sample			
	DP25	AHR	SAA	SAR
DRS bandgap (eV)	3.232 ± 0.003	3.248 ± 0.015	3.229 ± 0.014	3.018 ± 0.005
SEM-EDS contents (wt.%)	Ti = 59.9	Ti = 59.9	Ti = 59.9	Ti = 59.9
	O = 40.1	O = 40.1	O = 40.1	O = 40.1
XRD crystal phase composition (%)	Anatase = 85.3[a]	Anatase = 100	Anatase = 100	Anatase = 0
	Rutile = 14.7	Rutile = 0	(99.7)[b]	Rutile = 100
			Rutile = 0	(99.995)[b]
BET surface area (m^2 g^{-1})	50.5	10.2	32.4	0.4
Primary particle size (nm)	30[c]	_[d]	<25[b]	_[d]
Mean aggregate particle size in deionised water (μm)[e]	4.4	0.2	5.8	33.2
pH in deionised water	3.7	6.7	5.0	5.5

[a] Variable reports from literature [32–34].
[b] Provided by the supplier.
[c] From ref. [31].
[d] Not provided by the supplier.
[e] Determined using a Malvern Mastersizer 2000 instrument.

are highly coordinated with halides. In an earlier study we have reported this fact, i.e. the inability to photocatalytically reduce a highly chloride coordinated noble metal, together with the first published evidence of the ability to photocatalytically reduce lower chloride coordinated noble metal species in the absence of an added SRA [23]. This study is an extension of that work and focuses on the photocatalytic behaviour of four different TiO$_2$ powders for the photocatalytic reduction of the aqueous $[PdCl_n(H_2O)_{4-n}]^{2-n}$ – system, again in the absence of an added SRA. The four TiO$_2$ powders exhibit different intrinsic parameters such as surface area, crystal phase composition, aggregate particle size and bandgap energies. These intrinsic parameters, together with extrinsic parameters like the structure of the $[PdCl_n(H_2O)_{4-n}]^{2-n}$ $n = (0–4)$ complexes, have been found to affect the rate of photocatalytic reactions [23–26]. Dissolved oxygen, adsorbed on the surface of titanium dioxide, is an important parameter affecting the photocatalytic reduction process, as it acts as an electron acceptor and therefore competes with the dissolved Pd(II)-species for the excited electron, thereby affecting the rate of metal reduction [23,27]. With this in mind, an investigation was conducted to ascertain the extent to which oxygen influences the photocatalytic reduction of chloroaqua Pd(II) complexes. We report here for the first time the ability to photocatalytically reduce a highly chloride coordinated noble metal species, i.e. $[PdCl_4]^{2-}$, in the absence of an added sacrificial reducing agent.

2. Experimental

2.1. Chemicals and preparation of individual chloro-aqua palladium(II) complexes

The detailed procedure for making up the different solutions is reported in our earlier communication [23]. This involved making up individual solutions (at constant ionic strength and pH) at the specific pCl-value that coincides with the maximum concentration of each Pd(II) species, employing the distribution diagram for the $[PdCl_n(H_2O)_{4-n}]^{2-n}$ ($n = 0–4$) system. The palladium sponge (99.9% purity) used to prepare the stock solution was sourced from Sigma–Aldrich as well as NaCl (99.98%) and NaClO$_4$·H$_2$O (analytical grade). HClO$_4$ (70%) and HNO$_3$ (100%) were obtained from Merck. Deionised water from a Millipore Milli-Q system was used to prepare all solutions. Four commercially available titanium dioxide powders were employed as photocatalysts for this study. These are Degussa P25 (DP25) supplied by Evonik Industries, Tioxide A-HR (AHR) provided by Tioxide Southern Africa (Pty) Ltd, Sigma–Aldrich Anatase (SAA), and Sigma–Aldrich Rutile (SAR).

2.2. Photocatalyst characterisation

The physicochemical properties of the four titanium dioxide samples are summarised in Table 1. The atomic composition was determined employing a FEI Quanta 200 ESEM with an Oxford X-sight EDS detector using INCA software and it is clear that all four samples exhibit the same atomic composition. The band gap energies of the photocatalysts were determined employing the Kubelka–Munk function [28–30] and UV–VIS Diffuse Reflectance Spectroscopy (DRS) measurements on an Analytik Jena SPECORD S600 spectrophotometer using WinASPECT software. The crystal phase composition of the samples was determined employing a X'Pert Pro diffractometer (Model: PW3040/60). The BET surface area was determined employing a Micromeritics ASAP 2020 instrument, while the mean aggregate particle size of the dispersed powders in water was determined employing a Malvern Mastersizer 2000 instrument. The AHR sample is a versatile pigment that finds a wide range of specialist applications from paper to ceramics. It is a 100% anatase powder as determined by X-ray diffraction, free from oversize particles and self-dispersing in water. Its BET surface area is 10.2 m^2 g^{-1} and it has by far the smallest mean aggregate particle size of 0.2 μm when dispersed in deionised water. The SAR sample, consisting of 100% rutile, has the smallest BET surface area of 0.4 m^2 g^{-1} and the largest mean aggregate particle size of 33 μm in deionised water. SAA, a 100% anatase material, has a BET surface area of 32.4 m^2 g^{-1} while the DP25 sample with a BET surface area of 50.5 m^2 g^{-1} has a crystal phase composition of 85.3% anatase and 14.7% rutile. The DP25 sample is generally taken as the standard against which other photocatalysts are compared [31]. Although the degree of aggregation of the samples in deionised water is an intrinsic parameter, it is influenced by the reaction solution pH and therefore affects the adsorption of molecules, photon absorption and light scattering [24]. All the photocatalyst samples were used without any pre-treatment.

2.3. Batch experimental procedure

Photocatalytic reduction experiments were carried out in a batch reactor shown in Fig. 1. It consisted of a jacketed cylindrical glass reactor vessel with an external height of 20.3 cm, an internal height of 18.5 cm, an external diameter of 9.5 cm, and an internal diameter of 7 cm. A Philips TUV PL-S 9W/2P compact UVC germicidal fluorescent lamp within a quartz glass housing, with a peak emission at 254 nm, was employed as the UV source and placed at the centre of the photoreactor. To prevent the unnecessary loss of UV light through scattering, as well as illumination
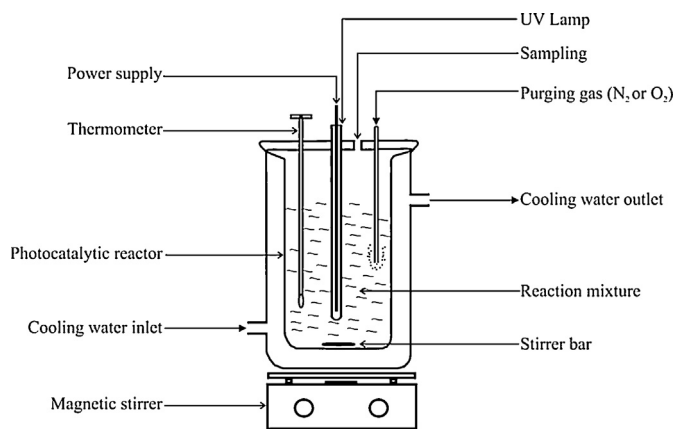
Fig. 1. Cross-section of the batch photocatalytic reduction apparatus.

of the suspension by ambient light, the reactor was covered on the outside by aluminium foil and black duct tape. A 500 ml solution containing the dominant chloro-aqua palladium(II) complex of interest was freshly prepared prior to each experimental run. The solution temperature was maintained at 25 °C employing a Julabo F12 ED refrigerated thermostat and monitored using a glass mercury thermometer. Three reaction 'atmospheres' were employed, i.e. medical grade oxygen, ambient air and analytic grade nitrogen (to remove dissolved oxygen). For those runs where nitrogen or oxygen was purged, the solutions were purged for 30 min prior to illumination and continuously thereafter for the duration of the run. The amount of TiO_2 photocatalyst in suspension was $2\,g\,l^{-1}$. The reaction suspensions were continuously stirred for 30 min in the dark before illumination to allow for maximum photocatalyst dispersion and to ensure that equilibrium is reached with regard to the adsorption of reactants onto the TiO_2 photocatalyst surface. Stirring was maintained during each run to prevent the photocatalyst from settling and all experiments were conducted in the absence of an added organic sacrificial reducing agent (SRA). During a run of 150 min, 10 ml samples were taken from the reactor at 15-min intervals and subjected to double filtration employing Whatman grade 42 filter papers. Dissolved metal analyses were conducted by means of inductively coupled plasma (ICP) emission spectroscopy employing a Thermo iCAP 6300 instrument. Palladium removal is shown as a normalised concentration, that is, the instantaneous Pd(II) filtrate concentration (C) divided by the initial Pd(II) concentration (C_0), which was 50 ppm for all runs. The observed photocatalytic reduction trends are the mean of three repeats as shown by the calculated standard errors for each sample point.

3. Results and discussion

3.1. Thermodynamic analysis and the photocatalytic redox principle of $[PdCl_n(H_2O)_{4-n}]^{2-n}$ (n = 0–4) species in an aqueous solution

Eqs. (1)–(5) show the calculated standard reduction potentials of the five chloro-aqua palladium(II) complexes [23,37]. Thermodynamically, these complexes are stable in water and are not reduced by H_2O under normal conditions (in the absence of a catalyst). From these standard reduction potentials one would expect $[PdCl_4]^{2-}$ to be the least prone to reduction while $[Pd(H_2O)_4]^{2+}$ would be the easiest to reduce. Moreover, in this system, the reduction of dissolved oxygen (Eq. (6)) is a competing reaction with a far more favourable reduction potential of 1.229 V in acidic media under standard conditions. Therefore, in order to offset the negative effect

of dissolved oxygen during the photocatalytic reduction process an inert atmosphere (N_2) was employed.
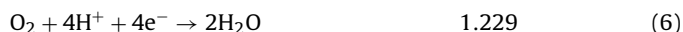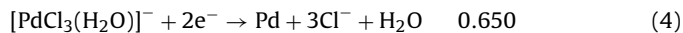
$$[Pd(H_2O)_4]^{2+} + 2e^- \rightarrow Pd + 4H_2O \qquad 0.951 \qquad (1)$$

$$[PdCl(H_2O)_3]^+ + 2e^- \rightarrow Pd + Cl^- + 3H_2O \qquad 0.819 \qquad (2)$$

$$PdCl_2(H_2O)_2 + 2e^- \rightarrow Pd + 2Cl^- + 2H_2O \qquad 0.721 \qquad (3)$$

$$[PdCl_3(H_2O)]^- + 2e^- \rightarrow Pd + 3Cl^- + H_2O \qquad 0.650 \qquad (4)$$

$$[PdCl_4]^{2-} + 2e^- \rightarrow Pd + 4Cl^- \qquad 0.610 \qquad (5)$$

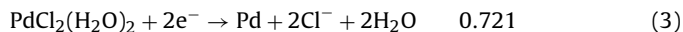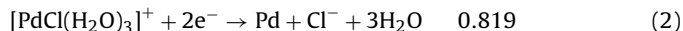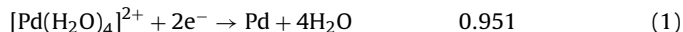$$O_2 + 4H^+ + 4e^- \rightarrow 2H_2O \qquad 1.229 \qquad (6)$$

Fig. 2 is a schematic illustration of the processes that take place on the surface of a TiO_2 particle after photo-excitation by UV light. As noted in literature [35], the arrows are not a representation of the migration of the species into the bulk solution but rather serve to indicate their fate on the photo-excited TiO_2 surface, which is in line with a true heterogeneous catalytic process. According to the diagram, charge separation occurs as a result of the absorption of an amount of energy (photons) greater than or equal to the bandgap of TiO_2 (3.2 eV for anatase and 3.0 eV for rutile). According to literature [36], a series of redox reactions subsequently occur on the photo-excited TiO_2 surface. These include conduction band electron trapping (preferably by Pd(II) species), electron–hole recombination and electron scavenging by dissolved oxygen. The resultant electron, which migrates to the surface of the semiconductor particle, either reduces the dissolved Pd(II) species to the metallic form, which gets deposited onto the TiO_2-particle, or it reduces dissolved oxygen to a highly reactive superoxide $O_2^{\bullet-}$. The positive hole, acting as an oxidising agent, requires an electron in order to restore neutrality to the particle, which, in most cases, is achieved by the addition of an SRA (or hole scavenger), most often in the form of an organic compound, e.g. ethanol, but neutrality can also be restored by electron–hole recombination. In the absence of an organic SRA, water, within the coordination sphere of the complexes and/or the bulk reaction solution, is oxidised to hydroxyl radicals. Since there is no organic material to oxidise, the hydroxyl radicals resulting from H_2O oxidation react with the superoxides to form hydroperoxyl radicals (Eq. (7)). The hydroperoxyl radicals are also electron scavengers, which give rise to peroxyl ions (Eq. (8)). In strongly acidic media, such as the case here, the peroxyl ions are protonated to hydrogen peroxide (Eq. (9)). In a solution of high acidity, H_2O_2 is expected to be more stable but the presence of Pd(II) ions at 25 °C accelerates its decomposition to oxygen and water according to Eq. (10).

These two products are recycled back into the system preventing electron–hole recombination. However, for as long as there is dissolved oxygen in the system the conduction band electron trapping by Pd(II) is impeded through the undesirable electron scavenging. The following sections discuss the photocatalytic reduction observations made on four different TiO_2 photocatalysts.
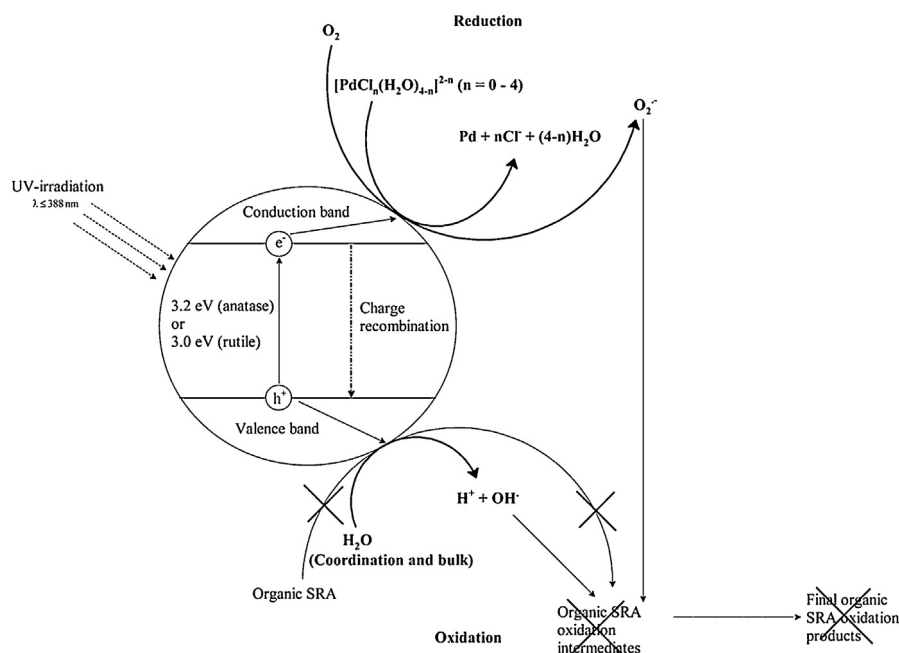
$$OH^\bullet + O_2^{\bullet-} \rightarrow HOO^\bullet \qquad (7)$$

$$HOO^\bullet + e^- \rightarrow HOO^- \qquad (8)$$

$$HOO^- + H^+ \rightarrow H_2O_2 \qquad (9)$$

$$2H_2O_2 \rightarrow 2H_2O + O_2 \qquad (10)$$

Fig. 2. Surface photocatalytic processes on TiO_2 during reduction of $[PdCl_n(H_2O)_{4-n}]^{2-n}$ ($n = 0–4$) complexes (adapted from [34]).

3.2. Photocatalytic reduction of $[PdCl_n(H_2O)_{4-n}]^{2-n}$ ($n = 0–4$) species over DP25

The time profiles of the normalised Pd(II) concentrations in the photocatalytic reduction of a $[PdCl_n(H_2O)_{4-n}]^{2-n}$ ($n = 0–4$) species on DP25 photocatalyst in oxygen, air and nitrogen are shown in Fig. 3. Oxygen has no significant impeding effect on the initial photocatalytic reduction rate of $[PdCl(H_2O)_3]^+$ and $PdCl_2(H_2O)_2$, but strongly affects the photocatalytic reduction of $[Pd(H_2O)_4]^{2+}$ and $[PdCl_3(H_2O)]^-$. No photocatalytic reduction was observed for the $[PdCl_4]^{2-}$ complex in all three atmospheres. The photocatalytic reduction of the neutral complex $PdCl_2(H_2O)_2$ proceeded to completion within 30 min in all instances. These results show that the rate of photocatalytic reduction of the neutral species is not influenced by oxygen (compare air and nitrogen purged solutions in the same figure) hence electron scavenging by oxygen at the surface of the excited TiO_2 particle does not effectively compete with electron transfer to the neutral Pd(II) species. Electron transfer to the neutral species is therefore a faster process compared to the overall oxygen reduction process, which is basically electron transfer to an oxygen molecule (Eqs. (6) and (11)). Since sampling was conducted at 15 min intervals, the fate of the complexes within the first 15 min is not known.

$$TiO_2(e^-, \ h^+) + Pd^{2+}_{adsorbed} \rightarrow TiO_2Pd^0(h^+) \qquad (11)$$
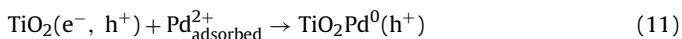
Thermodynamically, however, the reduction of oxygen in acidic media should be more favourable as dictated by the standard reduction potential of 1.229 eV (for oxygen reduction) compared to 0.721 eV for the reduction of $PdCl_2(H_2O)_2$ (Eqs. (3) and (6)) [37]. This confirms that the structure of the complex and surface properties of the photocatalyst play a crucial role in the photocatalytic reduction process [23].

3.3. Photocatalytic reduction of $[PdCl_n(H_2O)_{4-n}]^{2-n}$ ($n = 0–4$) species over AHR

Fig. 4 depicts the results of the photocatalytic reduction of $[PdCl_n(H_2O)_{4-n}]^{2-n}$ ($n = 0–4$) complexes over AHR. Unlike the case with DP25 photocatalyst, AHR shows a slower photocatalytic

reduction rate for the neutral $PdCl_2(H_2O)_2$ species compared to the cationic $[Pd(H_2O)_4]^{2+}$ and $[PdCl(H_2O)_3]^+$ complexes. The $[PdCl(H_2O)_3]^+$ complex is reduced within 15 min under N_2 and it is the fastest rate observed in this work. The anionic $[PdCl_3(H_2O)]^-$ and $[PdCl_4]^{2-}$ complexes do not reduce at all in pure oxygen and air. Further, the neutral species shows a slower initial reduction rate in air than in pure oxygen, which is somewhat surprising given that O_2 is easily reduced by the conduction band electrons thereby slowing down the photocatalytic reduction of $[PdCl_n(H_2O)_{4-n}]^{2-n}$ ($n = 0–4$) complexes.

This could point towards a comparatively poorer adsorption of oxygen on the AHR surface compared to DP25. This is also seen in that $[PdCl_3(H_2O)]^-$ is reduced at a higher rate on DP25 than on AHR in both air equilibrated and nitrogen purged solutions. The poorer adsorption of oxygen on AHR compared to that of DP25 is supported by the fact that AHR suspensions has a pH of almost 7, whereas that of DP25 is a lot more acidic with a pH of 3.7. Since it is known that the amount of O_2 in solution decreases with illumination time [23] one would expect that N_2 purging of the solution would increase the rate of photocatalytic reduction of the neutral $PdCl_2(H_2O)_2$ species to coincide with those of the fastest reducing cationic complexes. There is to a certain extent an increase in the amount of Pd(II) reduced with time but not as fast as the cationic complexes which have more coordinated water molecules in their spheres. These observations point to other factors involved in the photocatalytic reduction of $[PdCl_n(H_2O)_{4-n}]^{2-n}$ ($n = 0–4$) complexes besides the nature of the photocatalyst (bandgap energy, surface area and degree of aggregation). At pH 1 the ionisation state of TiO_2 is shown in Eq. (12) where it exists in a protonated form [38].

$$TiOH + H^+ \rightarrow TiOH_2^+ \qquad (12)$$
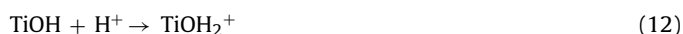
It is therefore expected that the anionic Pd(II)-complexes would adsorb better on the photocatalyst surface than the cationic complexes, but according to Fig. 4 the observed trend is cationic > neutral > anionic. This is in line with the fact that the anionic complexes have a more negative reduction potential and are therefore more difficult to reduce thermodynamically. This points towards the structure of the photocatalyst substrate playing
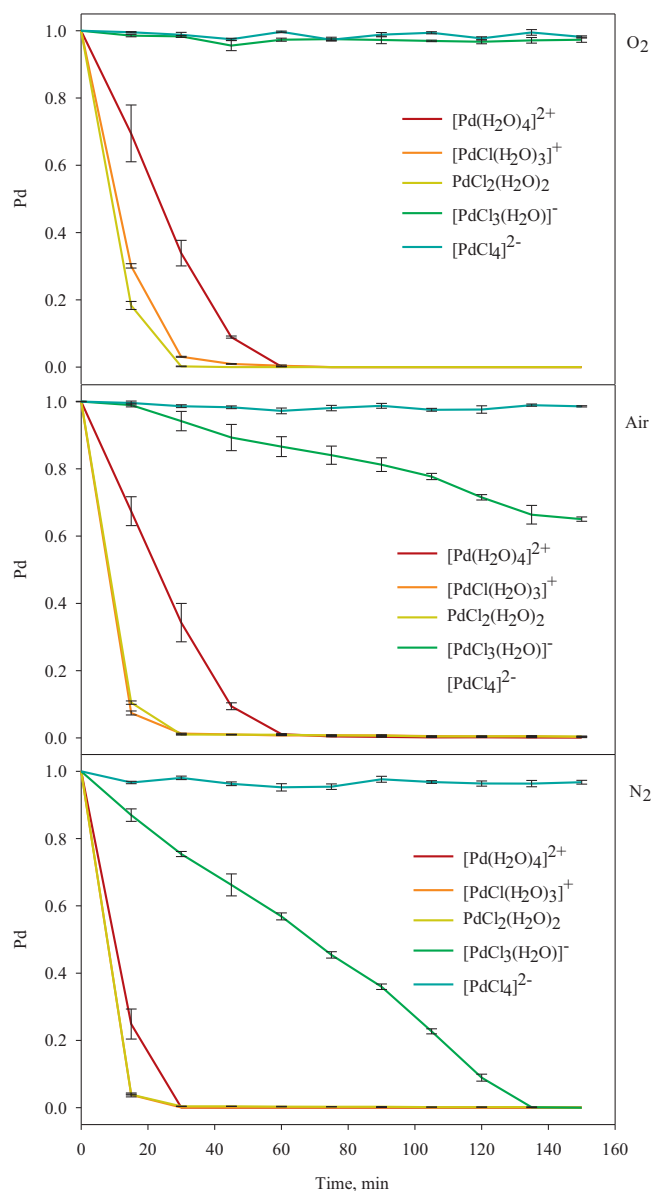
Fig. 3. Photocatalytic reduction of $[PdCl_n(H_2O)_{4-n}]^{2-n}$ ($n = 0$–4) employing DP25 TiO_2 for an oxygen purged, air equilibrated and nitrogen purged solution.

Fig. 4. Photocatalytic reduction of $[PdCl_n(H_2O)_{4-n}]^{2-n}$ ($n = 0$–4) employing AHR TiO_2 for an oxygen purged, air equilibrated and nitrogen purged solution.

a crucial role in the adsorption of oxygen and the subsequent photocatalytic reduction of the $[PdCl_n(H_2O)_{4-n}]^{2-n}$ ($n = 0$–4) complexes. It is also evident that, in general, the more coordination waters present within the sphere of the complex the faster its reduction will be on the AHR photocatalyst.

3.4. Photocatalytic reduction of $[PdCl_n(H_2O)_{4-n}]^{2-n}$ ($n = 0$–4) species over SAA

Fig. 5 shows the time profiles of the normalised Pd(II) concentration in the photocatalytic reduction of a $[PdCl_n(H_2O)_{4-n}]^{2-n}$ ($n = 0$–4) species on SAA photocatalyst. It is quite clear that SAA (a 100% anatase photocatalyst), in comparison to DP25, AHR, and SAR, was the least active for the photocatalytic reduction of the $[PdCl_n(H_2O)_{4-n}]^{2-n}$ ($n = 0$–4) complexes, in all three atmospheres, despite having a comparable bandgap energy and a relatively high BET surface area (Table 1).

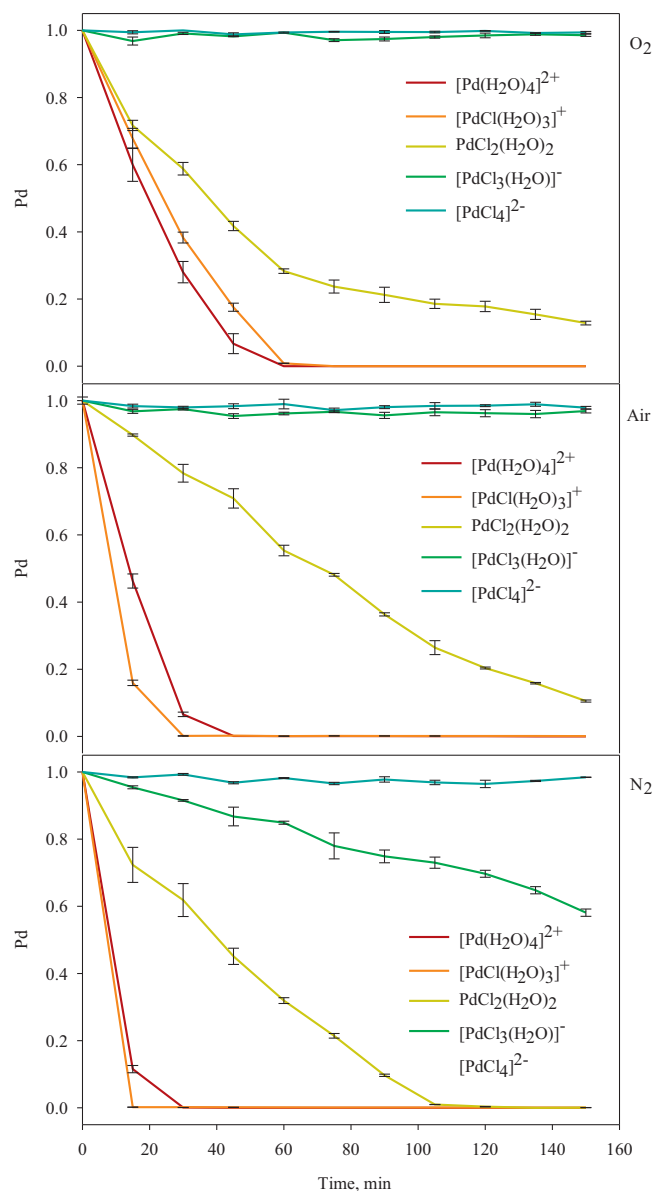This low activity could be due to (i) poor adsorption of the Pd(II)-complexes on the photocatalyst surface, resulting in poor surface coverage of the Pd(II)-complexes, which could be due to the poor intrinsic aggregation (dispersion) properties of SAA under the reported reaction conditions, and (ii) improved adsorption of oxygen, greater than that of AHR. It has been noted that one of the factors that affect adsorption is the nature of the exposed crystallographic facets of TiO_2 that have unsaturated surface atoms ready to bond with the adsorbent, thereby lowering the surface energy [24]. A further factor, also noted by the same authors, is the presence of competing ions in the system such as chlorides, nitrates and perchlorates. They are thought of as photocatalyst poisons that block the active sites resulting in the slowing down of the transfer of TiO_2 surface electrons to the complexes.

3.5. Photocatalytic reduction of $[PdCl_n(H_2O)_{4-n}]^{2-n}$ ($n = 0$–4) species over SAR

A surprising observation is that SAR (100% rutile), in both air and N_2, is the only photocatalyst capable of photocatalytically
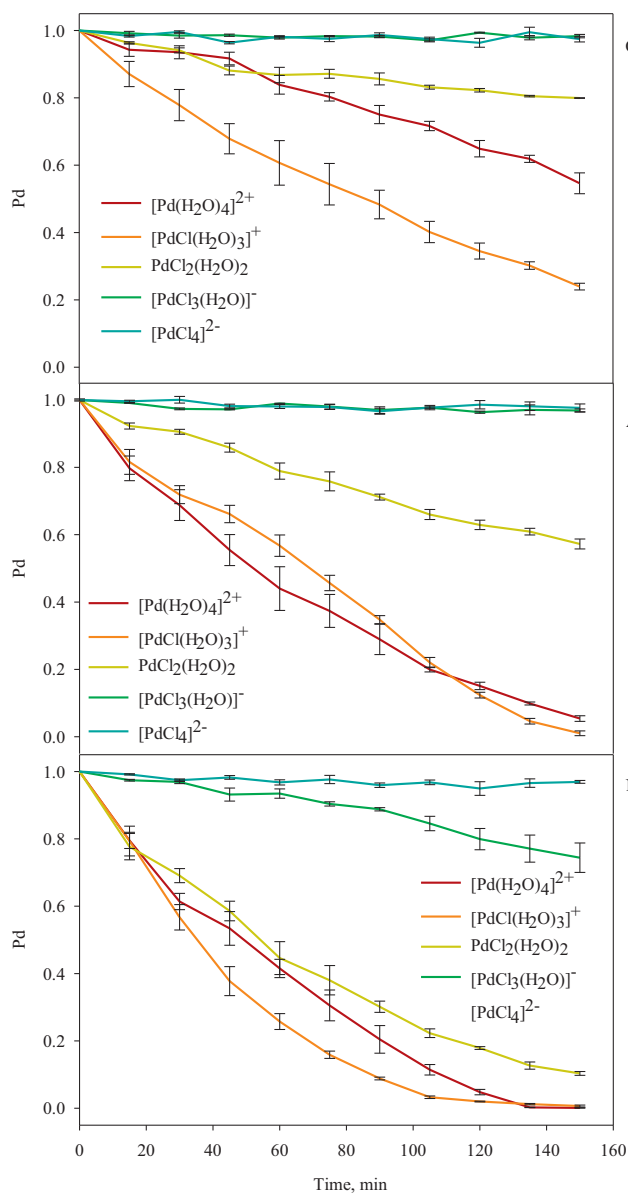
Fig. 5. Photocatalytic reduction of $[PdCl_n(H_2O)_{4-n}]^{2-n}$ ($n = 0$–4) employing SAA TiO$_2$ for an oxygen purged, air equilibrated and nitrogen purged solution.
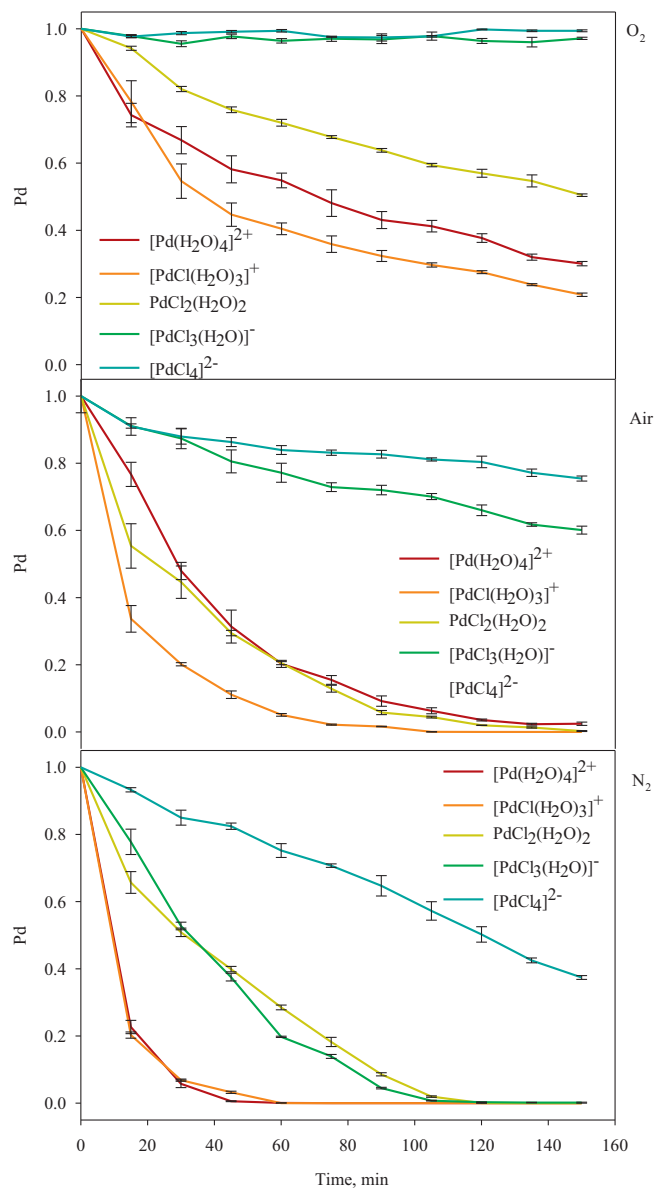

Fig. 6. Photocatalytic reduction of $[PdCl_n(H_2O)_{4-n}]^{2-n}$ ($n = 0$–4) employing SAR TiO$_2$ for an oxygen purged, air equilibrated and nitrogen purged solution.

reducing the $[PdCl_4]^{2-}$ complex, which is thermodynamically the most difficult to reduce (Fig. 6). One can however not state that oxygen adsorption is poor on SAR, as the lower chloride coordinated complexes are not reduced at a faster rate on SAR compared to for example DP25. There is therefore a change in the mechanism of the light-induced photocatalytic reduction of the complex on pure rutile compared to that on anatase. The differences in the photocatalytic activity of rutile SAR compared to the three anatase containing photocatalysts can be attributed to the differences in their physicochemical properties, especially the optical properties. Since the band gap energy for rutile is 3.02 eV compared to 3.2 eV for anatase, one would expect it to be less active than the anatase containing photocatalysts, under UV irradiation in these conditions, because of the anticipated quicker electron–hole recombination. However, this is not the case in the photocatalytic reduction of $[PdCl_n(H_2O)_{4-n}]^{2-n}$ ($n = 0$–4) complexes, specifically the $[PdCl_4]^{2-}$ complex. A review paper by Ni et al. [39] and references therein reported that the noble metals Pt, Pd and Rh are effective in

enhancing the photocatalytic ability of TiO$_2$. As the Fermi levels of these metals are lower than that of TiO$_2$, photo-excited electrons can be transferred from the conduction band to the metal particles deposited on the surface of the photocatalyst. This was found to greatly reduce the possibility of electron–hole recombination resulting in efficient separation and better photocatalytic reactions. The photogenerated electrons are immobilised in these surface traps before being scavenged by electron acceptors such as Pd(II) and oxygen. If oxygen is continuously bubbled through the reaction mixture then the opportunity for the above mentioned to occur is greatly reduced and no photocatalytic reduction of Pd(II) takes place.

Sun et al. [40], reported that differences in the oxygen sorption capacities of anatase and rutile can be critical in determining the photocatalytic activity. They mention that in the presence of Ag(I) or Fe(III), rutile appears more active than anatase for water splitting than for the photocatalytic degradation of organic compounds. Sclafani et al. [41] also observed poor O$_2$ adsorption capacity on their rutile sample, and these observations can explain why there

could be a higher affinity for $[PdCl_4]^{2-}$ than O_2 on SAR rutile in aqueous solution compared to anatase. Ryu and Choi [42] compared the photocatalytic activity of different TiO_2 samples towards the degradation rates of different organic pollutants/substrates. These samples included Degussa P25 as well as pure anatase and pure rutile samples and they observed that each of the TiO_2 samples exhibited a superior activity towards the degradation of at least one of the test-substrates. The comparison of the photocatalytic activities of anatase and rutile, based solely on their physicochemical properties, is therefore not straightforward as they are substrate specific. In our case the different $[PdCl_n(H_2O)_{4-n}]^{2-n}$ ($n = 0$–4) complexes are the different substrates that interact differently with the different photocatalysts. Ryu and Choi [42] states that, based on their data, the common belief that anatase is more photocatalytically active than rutile cannot be fully supported, which supports our observations. Different TiO_2 samples interact differently with the substrate under investigation as well as with O_2, which result in different photo-oxidation or photo-reduction rates.

3.6. Comparative illustration of the photocatalytic reduction of $[PdCl_n(H_2O)_{4-n}]^{2-n}$ ($n = 0$–4) species over DP25, AHR, SAA and SAR in the first 30 min of reaction

The SAR photocatalyst surpasses all others in its ability to photocatalytically reduce the anionic complexes $[PdCl_3(H_2O)]^-$ and $[PdCl_4]^{2-}$ in air and nitrogen (Fig. 7). Addition of chlorides to the $[PdCl_n(H_2O)_{4-n}]^{2-n}$ ($n = 0$–4) system to form the $[PdCl_4]^{2-}$ complex results in no observable photocatalytic reduction on DP25, AHR and SAA in all the three atmospheres, with reduction only taking place on rutile SAR in both air and nitrogen. Although the rates of reduction of the $[PdCl_4]^{2-}$ complex in air and nitrogen is slower than that of a solution where $[PdCl_3(H_2O)]^-$ complex dominates, the result shows that the efficiency of the photocatalytic reaction is increased by the palladium particles deposited on the SAR semiconductor surface. In the work by Erzsébet Szabó-Bárdos et al. [43] it was found that silver deposition on DP25 leads to a considerable change of the adsorption characteristics of the semiconductor resulting in a decrease of the band gap and an associated shift in its absorption spectrum to the visible region. However, the same authors noted that due to the electronic interaction occurring at the contact region between metal deposits and the semiconductor surface the electrons are removed from TiO_2 into the vicinity of metal particle resulting in the formation of Schottky barriers.

This leads to an efficient charge separation of the light generated (e^-_{cb}–h^+_{vb}) and therefore more effective electron transfer to the electron acceptors adsorbed on the surface of the particle than in the case of the pure TiO_2 without any metal doping. This explanation is more likely to be the case in the photocatalytic reduction of $[PdCl_4]^{2-}$ complex in air and nitrogen. The slowing down of the rate of photocatalytic reduction of $[PdCl_n(H_2O)_{4-n}]^{2-n}$ ($n = 0$–4) species with increasing chloride concentration may be due to less active sites available on titanium dioxide photocatalyst [44] in conjunction with the complexes being less prone to reduce due to their decreasing reduction potentials. The higher concentration of chloride in solution results in the blocking of titanium dioxide active sites, which are positively charged at pH 1. This is a probable explanation as to why the $[PdCl_4]^{2-}$ complex is resistant to photocatalytic reduction on the other three photocatalysts. It is well known that the efficiency of photocatalytic reduction is determined by the rate of the photogenerated electron–hole recombination. To increase the lifetime and/or maintain the charge separation (e^-_{cb}–h^+_{vb}) on the titanium dioxide photocatalyst, Sacrificial Reducing Agents (SRAs) also known as hole scavengers
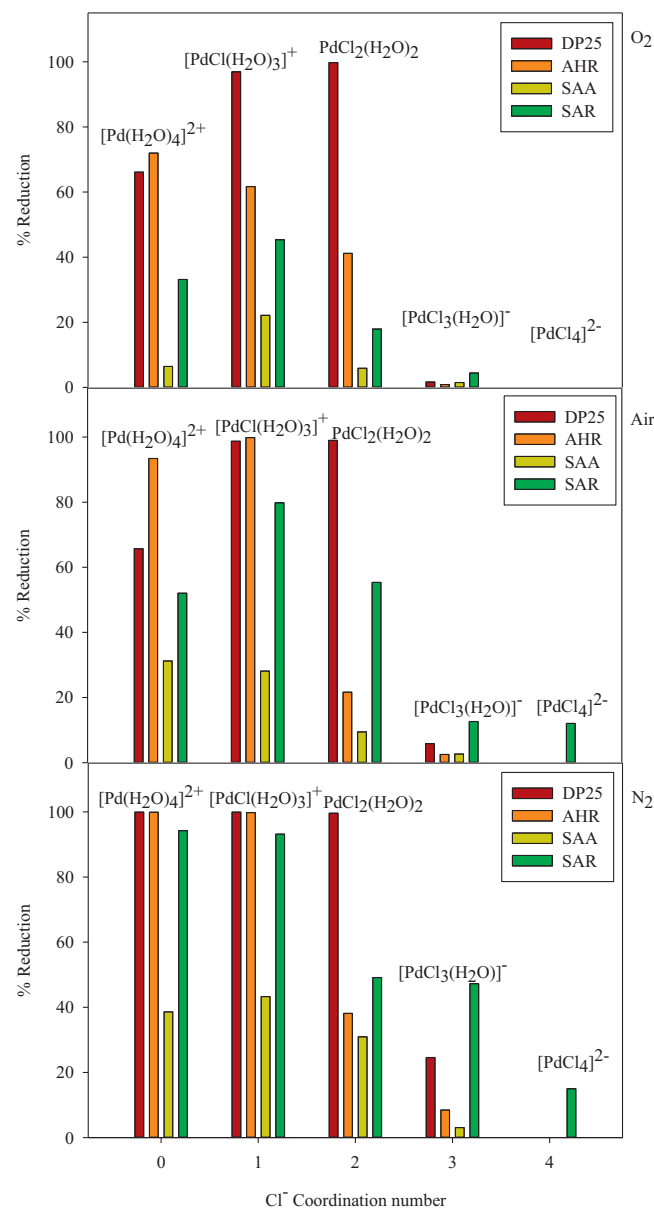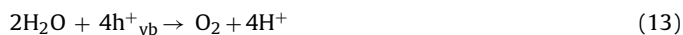

Fig. 7. Comparative photocatalytic reduction of $[PdCl_n(H_2O)_{4-n}]^{2-n}$ ($n = 0$–4) for an oxygen purged, air equilibrated and nitrogen purged solution in the first 30 min of irradiation.

in the form of organic compounds are usually employed [45]. However, with the knowledge of palladium speciation in aqueous solutions [23] an SRA may not be required in dilute waste water purification by photocatalysis. In this case, water acts as an SRA according to Equation 13 [41,46].

$$2H_2O + 4h^+_{vb} \rightarrow O_2 + 4H^+ \qquad (13)$$

From Fig. 7 and Table 1 it can be seen that the BET surface area had a secondary role in photocatalytic reduction of some of the $[PdCl_n(H_2O)_{4-n}]^{2-n}$ ($n = 0$–4) complexes because AHR with a $10.2\,m^2\,g^{-1}$ surface area was more active than DP25 in air, which has surface area of $50.5\,m^2\,g^{-1}$. Similarly, SAR with a BET surface area of $0.4\,m^2\,g^{-1}$ was more active than SAA in all instances, having a surface area of $32.4\,m^2\,g^{-1}$. From the analysis it is clear that the perceived discrepancies, based on the premise that anatase is more active than rutile, involves parameters other than the physicochemical properties of the photocatalysts. These parameters

include photocatalyst substrate interaction and oxygen adsorption capacities.

3.7. Adsorption (dark test) of the $[PdCl_n(H_2O)_{4-n}]^{2-n}$ (n = 0–4) complexes on the 4 photocatalysts

Experiments were carried out in the dark (under the same conditions as in the photocatalytic reduction runs) to probe whether adsorption of $[PdCl_n(H_2O)_{4-n}]^{2-n}$ complexes ($n = 0$–4) onto the four titanium dioxide photocatalysts would occur. Results (not shown) revealed that adsorption of the complexes did not take place and a decrease in the palladium concentration was not observed after 150 min for each of the four photocatalysts. Blank experiments or photolysis of the complexes also confirmed the fact that for photocatalytic reduction to take place both the photocatalyst and UV light are required.

4. Conclusions

Chloride ions in aqueous media combine with palladium(II) to form various chloro-aqua palladium(II) complexes, which vary in their predominance in solution depending on the concentration of chloride ions. The photocatalytic reduction of these species was carried out in titanium dioxide suspensions in a batch reactor at constant temperature, photocatalyst loading, pH and ionic strength on four photocatalysts in the absence of an organic sacrificial reducing agent (SRA). Highest rates of photocatalytic reduction were observed for the lower chlorinated Pd(II) species in air, nitrogen and pure oxygen. A significant decrease in the photocatalytic reduction rate of Pd(II) was observed as chloride concentration increased on all the four photocatalysts. In a solution where the neutral $PdCl_2(H_2O)_2$ complex dominates the rate of photocatalytic reduction is independent of the reaction atmosphere for the Degussa P25 photocatalyst. A 100% Sigma–Aldrich Rutile photocatalyst was the only one active in reducing highly chlorinated Pd(II) complexes, which can be of practical importance in the recovery of Pd(II) from effluent solutions as no additional SRA is required in the process. In general it has been observed that an increase in dissolved oxygen impedes the rate of photocatalytic reduction of all complexes on all photocatalyst surfaces. There was, however, no clear relationship between photocatalyst surface area and mean aggregate particle size on the rate of photocatalytic reduction. The rate of photocatalytic reduction strongly depends on the chloro-aqua Pd(II) complex dominant in an aqueous solution, i.e. the interaction of the complex with the surface of the photocatalyst, as well as the adsorption capacity of oxygen on the surface of the photocatalyst.

Acknowledgements

References

[1] J. Butler, S. Coles, M. Chung, K. White, Platinum Metals Review 55 (1) (2011) 41–42.
[2] J. Butler, S. Coles, M. Chung, K. White, Platinum Metals Review 55 (3) (2011) 153.
[3] D. Garwood, A. Cowley, M. Ryan, Platinum 2011, Johnson Matthey PLC (2011) 39–57.
[4] A. Zapf, M. Beller, Topics in Catalysis 19 (1) (2002) 77–78.
[5] J. Butler, Platinum Interim Review (2012) 1–44.
[6] P. Charlesworth, Platinum Metals Review 25 (1) (1981) 106–112.
[7] R. Gaita, S.J. Al-Bazi, Talanta 42 (2) (1995) 249–255.
[8] D.Jimenez de Aberasturi, R. Pinedo, I. Ruiz de Larramendi, J.I. Ruiz de Larramendi, T. Rojo, Minerals Engineering 24 (2011) 505–513.
[9] F.L. Bernardis, R.A. Grant, D.C. Sherrington, Reactive and Functional Polymers 65 (2005) 205–217.
[10] Z. Hubicki, A. Wolowicz, M. Leszczynska, Journal of Hazardous Materials 159 (2008) 280–286.
[11] Z. Hubicki, A. Wolowicz, M. Wawrzkiewicz, Chemical Engineering Journal 150 (2009) 96–103.
[12] L.I. Elding, L.F. Olsson, Journal of Physical Chemistry 82 (1) (1978) 69–74.
[13] C.D. Tait, D.R. Janecky, P.S.Z. Rogers, Geochimica et Cosmochimica Acta 55 (1991) 1253–1264.
[14] J.J. Cruywagen, R.J. Kriek, Journal of Coordination Chemistry 60 (4) (2007) 439–447.
[15] A. Wołowicz, Z. Hubicki, Solvent Extraction and Ion Exchange 28 (2010) 124–159.
[16] Z. Hubicki, A. Wołowicz, Hydrometallurgy 96 (2009) 159–165.
[17] A. Wołowicz, J. Zbigniew Hubicki, Chemical Engineering 152 (2009) 72–79.
[18] S.K. Lee, A. Mills, Platinum Metals Review 47 (2) (2003) 61–72.
[19] E. Borgarello, N. Serpone, G. Emo, R. Harris, E. Pelizzetti, Inorganic Chemistry 25 (1986) 4499–4503.
[20] R.J. Kriek, W.J. Engelbrecht, J.J. Cruywagen, Journal of the South African Institute of Mining and Metallurgy 95 (2) (1995) 75–81.
[21] J. Papp, H.S. Shen, R. Kershaw, K. Dwight, A. Wold, Chemistry of Materials 5 (1993) 284–288.
[22] H. Yoneyama, N. Nishimura, Hideo Tamura, Journal of Physical Chemistry 85 (3) (1981) 268–272.
[23] R.J. Kriek, F. Mahlamvana, Applied Catalysis A-General 423–424 (2012) 28–33.
[24] D. Friedmann, C. Mendive, D. Bahnemann, Applied Catalysis B: Environmental 99 (2010) 398–406.
[25] B. Ohtani, O.-O. Prieto-Mahaney, F. Amano, N. Murakami, R. Abe, Journal of Advanced Oxidation Technologies 13 (2010) 247.
[26] O.-O. Prieto-Mahaney, N. Murakami, R. Abe, B. Ohtani, Chemistry Letters 38 (2009) 238.
[27] D. Chen, A.K. Ray, Chemical Engineering Science 56 (2001) 1561–1570.
[28] B. Ohtani, Journal of Photochemistry and Photobiology C 11 (2010) 157–178.
[29] A.B. Murphy, Solar Energy Materials and Solar Cells 91 (2007) 1326–1337.
[30] K.M. Reddy, S.V. Manoram, A.R. Reddy, Materials Chemistry and Physics 78 (2002) 239–245.
[31] V.N.H. Nguyen, R. Amal, D. Beydoun, Chemical Engineering Science 60 (2005) 5759–5769.
[32] S. Bakardjieva, J. Subrt, V. Stengl, M.J. Dianez, M.J. Sayagues, Applied Catalysis B: Environmental 58 (2005) 193–202.
[33] N. Bowering, G.S. Walker, P.G. Harrison, Applied Catalysis B: Environmental 62 (2006) 208–216.
[34] T. Tan, D. Beydoun, R. Amal, Journal of Photochemistry and Photobiology A: Chemistry 159 (2003) 273–280.
[35] J-M. Herrmann, Applied Catalysis B: Environmental 99 (2010) 461–468.
[36] M.N. Chong, B. Jin, C.W.K. Chow, C. Saint, Water Research 44 (2010) 2997–3027.
[37] D.R. Lide, CRC Handbook of Chemistry and Physics, vol. 8(20–30), 87th ed., CRC Press, Boca Raton, Florida, US, 2006–2007.
[38] M. Qamar, M. Muneer, Desalination 249 (2009) 535–540.
[39] M. Ni, M.K.H. Leung, D.Y.C. Leung, K. Sumathy, Renewable and Sustainable Energy Reviews 11 (2007) 401–425.
[40] Q. Sun, Y. Xu, Journal of Physical Chemistry C 114 (2010) 18911–18918.
[41] A. Scaflani, J.M. Herrmann, Journal of Physical Chemistry 100 (32) (1996) 13655–13661.
[42] J. Ryu, W. Choi, Environmental Science and Technology 42 (2008) 294–300.
[43] E. Szabó-Bárdos, H. Czili, A. Horváth, Journal of Photochemistry and Photobiology A: Chemistry 154 (2003) 195–201.
[44] X. Wang, S.O. Pehkonen, A.K. Ray, Electrochimica Acta 49 (2004) 1435–1444.
[45] N.S. Foster, A.N. Lancaster, R.D. Noble, C.A. Koval, Industrial and Engineering Chemistry Research 34 (11) (1995) 3865–3871.
[46] M.I. Litter, Applied Catalysis B: Environmental 23 (1999) 89–114.